Photon-Gated Holography: Triphenylene in a Boric Acid Glass†

Antonio N. Russu,‡ Eric Vauthey, Changjiang Wei,§ and Urs P. Wild*

Physical Chemistry Laboratory, Swiss Federal Institute of Technology, ETH-Zentrum, CH-8092 Zürich, Switzerland *(Received: July 11, 1991)*

The observation of photon-gated hologram formation in a boric acid glass doped with triphenylene is reported. The first photon excites triphenylene to its first singlet excited state and, through intersystem-crossing, populates the first triplet state T_1. The second photon excites T_1 to T_n, where autoionization occurs, leading to the formation of a radical cation. The gating light populating T_1 via S_1 is spatially uniform, while the light exciting T_1 to T_n is spatially modulated. The long lifetime of the first triplet state allows recording with low light intensities (mW/cm^2). The spatially modulated excitation light forms three gratings (educt, intermediate state, and product). The extent of the interaction between these gratings depends on the overlap between educt, intermediate, and product absorption and refraction spectra as well as on the reading wavelength. The holograms were read at 363.8 and 632.8 nm. When the gating light is blocked, the holographic efficiency stays constant when read at 632.8 nm but increases substantially when read at 363.8 nm.

Introduction

Optical holography is a sensitive technique to investigate photochemical and photophysical processes in solids. For real-time applications, self-developing holographic recording materials are required. Biphotonic processes, in which two energetically different photons are used in the writing step, are especially well suited for this application. Only one photon is necessary to read the hologram, inducing no further photochemistry and facilitating repeated reconstructions without degradation. Since the fundamental work of Lewis and Kasha,[1] triplet states of organic molecules in glasses have been known to be relatively long-lived intermediates. Several systems[2-6] allowing nondestructive reading have already been found: for example, carbazole in poly(methyl methacrylate) and diacetyl in poly(α-cyanoacrylate). In both cases, the intermediate triplet state absorbs the second photon. As the triplet lifetime of these compounds is still relatively short (55 μs for diacetyl[7]), high light intensities (1-100 W/cm^2) are required for efficient writing. For practical reasons, it would be much more convenient to find materials with an efficient biphotonic reaction at lower intensities. One way to achieve this is to choose a system with a really long-lived triplet state, thus increasing the probability of absorbing the second photon.

The interference pattern of the writing beams leads to a spatially modulated photoproduct concentration, thus forming a grating. In addition, the disappearing educt concentration is also modulated and its grating must also be considered. The maxima of the photoproduct concentration correspond to minima of the educt concentration. These concentration gratings thus have a phase difference of π. The total diffraction efficiency of the material is the sum of the contribution of the educt and the product gratings. If a transient intermediate state is formed with a substantial stationary concentration, its grating has also to be considered and can significantly increase or decrease the total diffraction efficiency.

In this paper we describe, to our knowledge, the first observation of biphotonic holographic recording with intensities of the order of 50 mW/cm^2. The material is boric acid glass doped with triphenylene. Boric acid glass was chosen as a host for its unique property of reducing the ionization potential of the guest molecule.[8] The ionization potential of triphenylene is lowered from 8.09 eV in the gas phase to 5.70 eV in boric acid glass.[9] The reaction mechanism involves a stepwise absorption of two photons (Figure 1). The first excites triphenylene to the first singlet excited state and, through intersystem crossing, populates the first triplet state T_1. The second photon excites T_1 to an upper excited triplet state T_n, where autoionization occurs,[9] leading to the formation of a radical cation. In our experiment, the light populating T_1 via S_1 is the gating light and is spatially uniform, while the light exciting T_1 to T_n is spatially modulated. The main features of this system are the long triplet lifetime of triphenylene in boric acid glass (τ = 10.7 s) and the lowering of the triphenylene ionization potential in boric acid glass (I = 5.70 eV[9]), allowing ionization in the triplet manifold with a near-UV photon.

Experimental Section

The samples were prepared by melting a mixture of triphenylene (Fluka, puriss.) and boric acid (Fluka, purum) at about 210 °C between two quartz plates. The resulting metaboric acid glasses were 0.10-0.15 mm thick and of good optical quality. The triphenylene concentration was spectroscopically measured to be about 10^{-3} M.

Figure 2 shows the experimental setup used to record and read the holograms. The UV-all lines output of an Ar^+ ion laser (Spectra Physics, Model 2045) was dispersed by a quartz prism into three groups of lines. The first group at 333.6, 334.5, and 335.8 nm (beam 1) was used as the spatially uniform gating beam to populate the triplet state. The middle group at 351.1 and 351.4 nm was blocked while the last group at 363.8 nm (beam 2) was split into two parts of equal intensity, a reference and an object beam, which were overlapped on the sample to generate a fringe pattern. The angle between the interfering beams was about 10°, resulting in a fringe spacing of approximately 1 μm. The spot diameter on the sample was about 5 mm.

In order to monitor the spatial phase of the grating, a small part of the reference and object beams was reflected from a quartz beam splitter mounted in front of the sample to create a second interference pattern. This pattern was expanded by combining a cylindrical lens with a diffraction grating at grazing incidence and detected by a Reticon photodiode array. The signal from the diode array was displayed on an oscilloscope and was monitored to ensure that no phase shift occurred during the hologram writing.

† Dedicated to Michael Kasha on the occasion of his 70th birthday.

‡ Present address: Dow Europe S.A., Bachtobelstrasse 3, CH-8810 Horgen, Switzerland.

§ Permanent address: Changchun Institute of Physics, Changchun, People's Republic of China.

(1) Lewis, G. N.; Kasha, M. *J. Am. Chem. Soc.* **1944**, *66*, 2100.
(2) Bräuchle, C.; Burland, D. M. *Angew. Chem., Int. Ed. Engl.* **1983**, *22*, 582 and references therein.
(3) Bjorklund, G. C.; Bräuchle, C.; Burland, D. M.; Alvarez, D. C. *Opt. Lett.* **1981**, *6*, 159.
(4) Schmitt, U.; Burland, D. M. *J. Phys. Chem.* **1983**, *87*, 720.
(5) Bräuchle, C.; Wild, U. P.; Burland, D. M.; Bjorklund, G. C.; Alvarez, D. C. *Opt. Lett.* **1982**, *7*, 177.
(6) Gerbig, V.; Grygier, R. K.; Burland, D. M.; Sincerbox, G. *Opt. Lett* **1983**, *8*, 404.
(7) Grygier, R. K.; Brugger, P. A.; Burland, D. M. *J. Phys. Chem.* **1985**, *89*, 112.
(8) Joussot-Dubien, J.; Lesclaux, L. *J. Chim. Phys.* **1964**, *61*, 1631.
(9) Andreev, O. M.; Smirnov, V. A.; Alfimov, M. V. *J. Photochem.* **1977**, *7*, 149.
(10) Labhart, H.; Heinzelmann, W. *Organic Molecular Photophysics*; Birks, J., Ed.; Wiley: New York, 1973; Vol. 1.

0022-3654/91/2095-10496$02.50/0

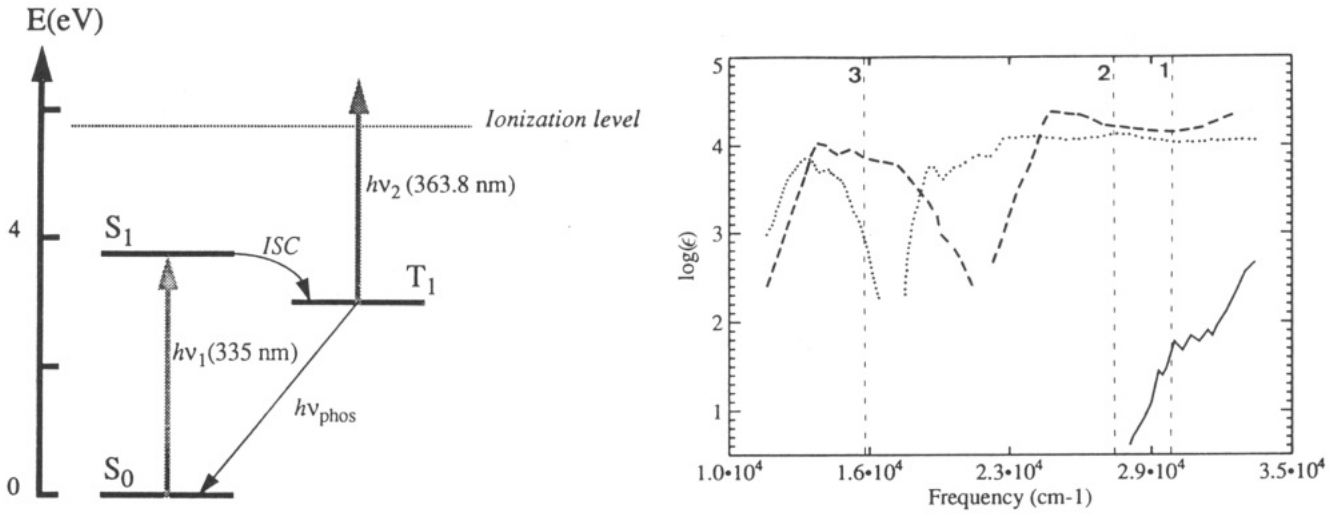

Figure 1. Energy diagram of the states involved in the biphotonic ionization of triphenylene in boric acid glass and UV/vis absorption spectra of the triphenylene ground state (full), triplet state (dashed, from ref 10), and radical cation (dotted). The vertical lines correspond to the wavelengths of beams 1–3.

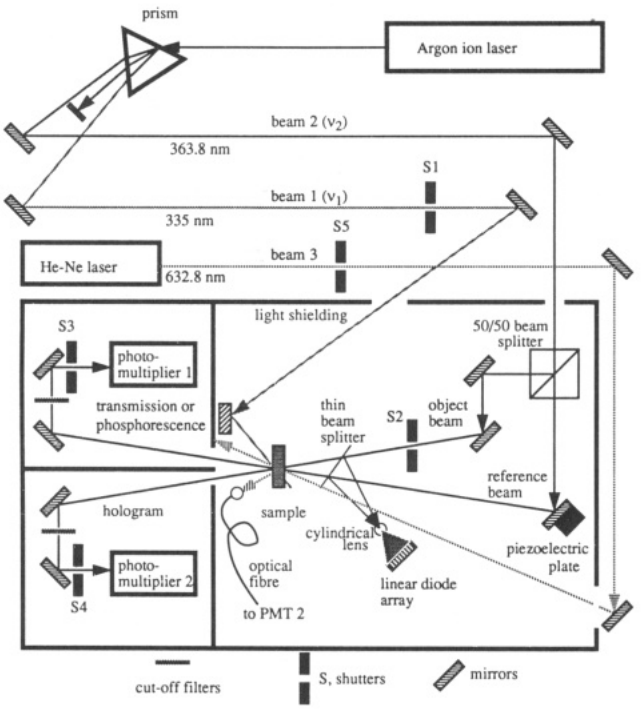

Figure 2. Experimental setup used to write and read holograms and to measure phosphorescence and transmission.

Deliberate spatial phase shifts of the grating pattern could be adjusted by monitoring the grating while moving a mirror mounted on the piezoelectric transducer.

The hologram efficiency was investigated at two different wavelengths. At the first (363.8 nm), the object beam was blocked and the intensity of the diffracted part of the reference beam was measured. Simultaneously, the phosphorescence or the transmission of the sample could be determined. Diffraction and either phosphorescence or transmission signals were detected by two photomultipliers (PM2 and PM1, respectively) connected to single-photon-counting electronics. The apertures of the photomultipliers were equipped with shutters which were closed during the writing process. All shutters were controlled by a DEC PDP11-23 computer. For the measurement of diffracted and transmitted light, UV-pass filters were placed in front of both photomultipliers in order to eliminate phosphorescence; for phosphorescence detection, the UV-pass filter on PM1 was replaced by cutoff filters absorbing all light below 400 nm.

At the second wavelength studied (632.8 nm), the hologram was read by a helium–neon laser (beam 3) (Spectra-Physics, Model 106-1, 10 mW) whose incidence angle was adjusted to satisfy the Bragg condition. The diffracted light was detected with PM2 equipped with filters which blocked all light below 600 nm. Typical diffraction efficiencies were of the order of 10^{-5}.

Theory

According to Kogelnik,[11] the diffraction efficiency of a plane wave hologram is given by

$$\eta = \frac{I_{dif}}{I_{inc}} = \left[\sin^2\left(\frac{\pi n_1 d}{\lambda \cos\theta}\right) + \sinh^2\left(\frac{\alpha_1}{2\cos\theta}\right)\right] \exp\left(-\frac{2\alpha_0}{\cos\theta}\right) \quad (1)$$

where d is the thickness of the sample, n_1 and α_1 are the modulation amplitudes of refractive index and optical density in the grating, θ the Bragg angle, λ the wavelength of the diffracted light, and α_0 the average optical density of the sample. The first Fourier coefficients of the series expressing the spatially periodic variation of optical density and refractive index are given by α_1 and n_1, respectively. In the initial phase of the hologram recording, these modulations are harmonic and higher order terms can be neglected. The first term in the square brackets describes the hologram formed as a result of changes in the refractive index: the so-called phase hologram. The second term is related to effects resulting from absorbance changes: the amplitude hologram. The exponential term accounts for the unmodulated absorption of the sample. If the absorption spectra of educt and product are well separated, the total modulation amplitude leading to the observed diffraction efficiency is due to either the educt grating or the product grating, depending on the wavelength of the diffracted light. On the other hand, if their spectra overlap, the contribution of both species to the absorption and index of refraction changes must be considered. In the present case, a long-lived intermediate state is also involved in the photochemical reaction and its concentration grating must also be taken into account.

The total modulation amplitudes α_1 and n_1 are

$$n_1 = n_1^{P} + n_1^{E} + n_1^{I} \quad (2)$$

$$\alpha_1 = \alpha_1^{P} + \alpha_1^{E} + \alpha_1^{I} \quad (3)$$

where the superscripts P, E, and I designate product, educt, and intermediate, respectively. As $\sin^2$ and $\sinh^2$ are both even functions, only the absolute values of n_1 and α_1 are significant. The amplitude of the absorption modulation is given by[12]

$$\alpha_1^{i} \cong \Delta\alpha_i = 2.303 d \epsilon_i \Delta C_i \quad (4)$$

(11) Kogelnik, H. *Bell System Tech. J.* **1969**, *48*, 2909.

TABLE I: Molar Extinction Coefficients ϵ (M^{-1} cm^{-1}) and Molar Refractions R (M^{-1}) of the Triphenylene Ground State (E), Triplet Excited State (I), and Radical Cation (P) at Both Reading Wavelengths

	363.8 nm	632.8 nm
ϵ_E	≈0	≈0
ϵ_I	16 800	500–2000
ϵ_P	24 000	14 200
R_E	0.4153	0.3286
R_I	0.4594	0.3340
R_P	0.4373	0.3347

where i may be E, I, or P and $\Delta\alpha_i$ is the optical density change due to concentration variation, ΔC_i, of i with an extinction coefficient ϵ_i.

In the same way, the refractive index modulation amplitude n_1 can be calculated using the following relation[12]

$$n_1^i \cong \Delta n_i = \frac{((n_0^i)^2 + 2)^2}{6n_0^i} R_i \Delta C_i \qquad (5)$$

where n_0^i and R_i are, respectively, the average refractive index and the molar refraction of E, I, or P. The molar refraction at a given wavelength can be calculated from the refractive index at that wavelength with the Lorentz–Lorenz relation.[13] The refractive index and the absorption are the real and the imaginary parts of the complex refractive index, respectively. Therefore, using the Kramers–Kronig relations, the refractive index can be obtained from the absorption.[14] After some transformations, the molar refraction itself can be calculated from the electronic absorption spectra of E, I, and P[15]

$$R_i(\lambda_0) = \frac{2303}{3\pi^2} \int \frac{\epsilon_i(\lambda)}{1 - (\lambda/\lambda_0)^2} d\lambda \qquad (6)$$

where the integral runs over all electronic absorption bands. In the present case, the educt E is the singlet ground state S_0, the long-lived intermediate I is the triplet state T_1, and the product P is the radical cation.

The extinction coefficients and molar refractions of triphenylene ground state, triplet, and cation at both reading wavelengths are given in Table I. These data show that the triphenylene ground state does not form an amplitude hologram at 363.8 and 632.8 nm, its extinction coefficient being zero at both wavelengths. Therefore, its contribution to the diffraction efficiency can originate only from its phase hologram.

Results

The absorption spectra of the triphenylene ground state, first excited triplet states, and radical cation are displayed in Figure 1; they indicate that the gating light at 335 nm (beam 1, ν_1) can excite the $S_1 \leftarrow S_0$ transition, while the light at 363.8 nm (beam 2, ν_2) is absorbed by the triplet state only.[10] In the first experiment, the gating light intensity was varied from 1 to 11 mW/cm². The intensity of the hologram forming beam was kept constant at 40 mW/cm². The formation of the hologram was monitored with a helium–neon laser at 632.8 nm (beam 3). The holographic growth curves are shown in Figure 3. The higher the intensity of beam 1, the faster the holographic efficiency rises and the earlier the maximum efficiency is reached. Two effects contribute to the subsequent reduction of efficiency as a function of time:

Two-photon ionization of triphenylene can take place with the gating beam alone (two 335-nm photons ≅7.4 eV). As the gating light is a single-plane wave, a spatially uniform product concentration is formed. The fringe contrast of the product grating

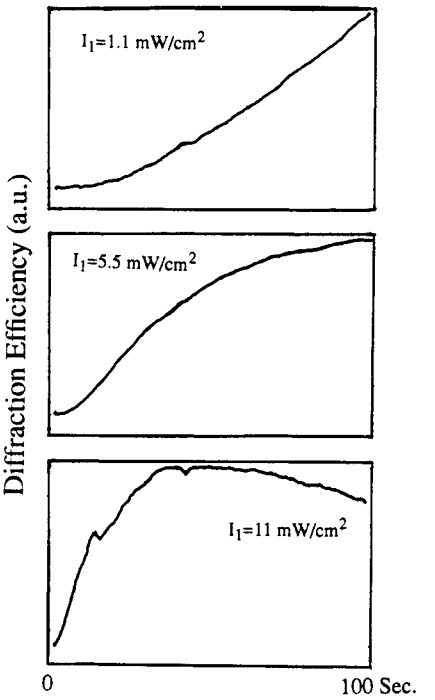

Figure 3. Holographic growth curves recorded with different gating light intensities I_1, with a constant intensity for the 363.8-nm beams (I_2 = 40 mW/cm²) and read at 632.8 nm.

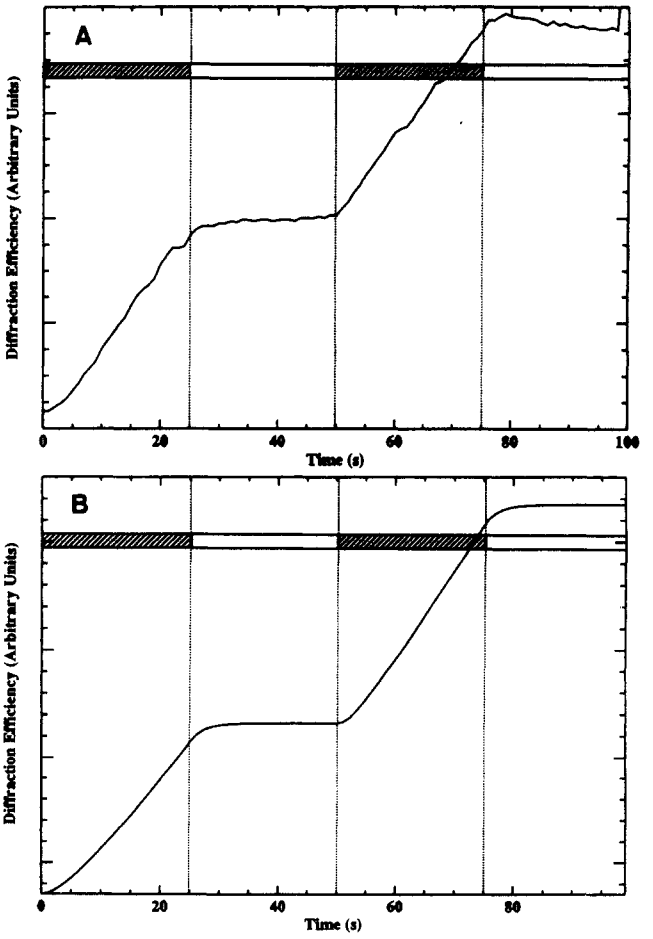

Figure 4. Measured (A) and calculated (B) holographic growth curves read at 632.8 nm with gating light on (dark) and off (white). I_1 = 1.5 mW/cm², I_2 = 80 mW/cm².

generated by the normal biphotonic process is decreased and the diffraction efficiency reduced.

The product concentration grating is harmonic only at the beginning of the photoreaction, but as the reaction proceeds, it

(12) Burland, D. M.; Bräuchle, C. *J. Chem. Phys.* **1982**, *78*, 4502.
(13) Tomlinson, B. J.; Chandross, E. A. *Adv. Photochem.* **1980**, *12*, 201.
(14) Jackson, J. D. *Classical Electrodynamics*; Wiley: New York, 1975; p 306.
(15) Deeg, F. W.; Pinsl, J.; Bräuchle, C.; Voitlander, J. *J. Chem. Phys.* **1983**, *79*, 1229.

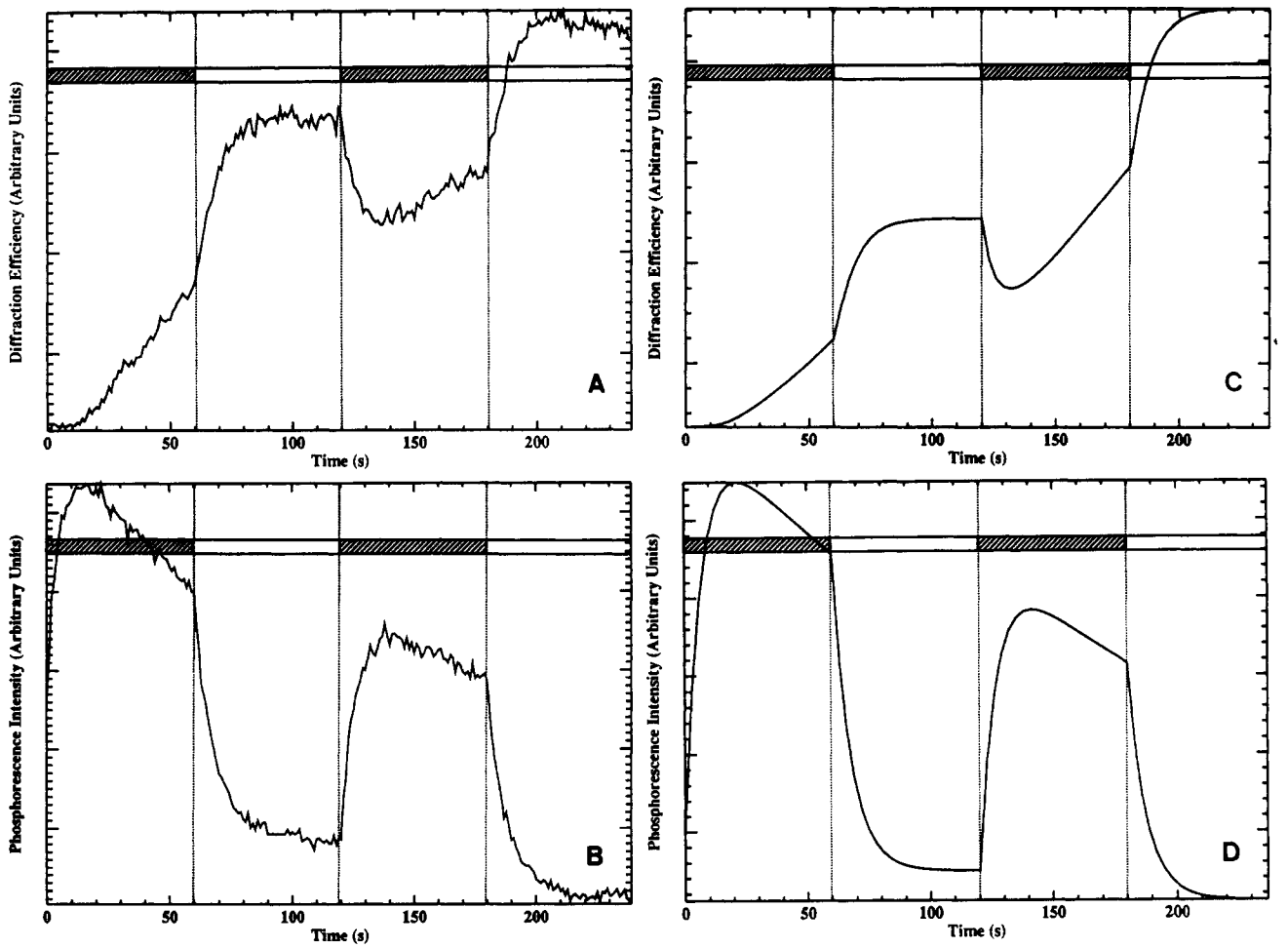

Figure 5. Measured (A) and calculated (C) holographic growth curves read at 363.8 nm with gating light on (dark) and off (white). I_1 = 6 mW/cm^2, I_2 = 80 mW/cm^2. Phosphorescence intensity measured simultaneously with the holographic growth curve (B) and calculated (D).

becomes more and more anharmonic and higher order holograms are formed. The first-order diffraction efficiency decreases.[16]

Figure 4A shows the result of an experiment that unambiguously demonstrates the effect of optical gating on hologram formation. During the first 25 s, the sample was exposed to the gating and holographic beams resulting in increasing diffraction efficiency. At t = 25 s, the gating beam was blocked and the hologram efficiency remains practically constant until the gating beam is opened again. For this experiment the hologram was read out with the He–Ne laser beam.

Figure 5A shows the result of a similar experiment but using the 363.8-nm reference beam for reading. During the first 60 s, the gating beam was on and the diffraction efficiency grows as for the He–Ne laser. After 60 s, the gating beam was blocked but now the efficiency rises abruptly until it reaches a maximum value at which it remains constant. This rise could be fitted to an exponential function with a time constant depending on the intensity of the 363.8-nm beam: the larger the intensity, the shorter the rise time. At t = 120 s, the gating beam shutter was reopened and the diffraction efficiency dropped quickly to a new minimum before increasing slowly again. The decrease could not be fitted to an exponential function as it depends in a complex way on the gating and hologram beam intensities. Triphenylene phosphorescence was measured simultaneously with the hologram growth curves (Figure 5B). With gating light on, the phosphorescence intensity increases rapidly to a maximum and then decreases slowly, the decay being at the same rate as the holographic growth with gating light on. In the same way as the holographic growth, the phosphorescence decay time decreases with increasing intensity of the 363.8-nm beam. This shows that the increase of diffraction efficiency involves triplet consumption.

(16) Meixner, A. J.; Renn, A.; Wild, U. P. *J. Chem. Phys.* **1989**, *91*, 6728.

Moreover, the sharp rise of phosphorescence behaves like the fast diffraction efficiency decay just after turning the gating light on. The time t_{max} at which the phosphorescence signal is maximum depends on the intensities of the gating and hologram beams: if the gating light intensity was increased compared to that of the hologram beams, t_{max} became shorter; on the other hand, when the gating light intensity was decreased, t_{max} was larger.

The results of a similar experiment but with a longer time scale and with different gating light intensities are displayed in Figure 6. The underlying behavior of the growth curve, ignoring the effect of turning on and off the gating light, is comparable to that observed when measuring with the He–Ne laser (Figure 3). The magnitude of efficiency change upon blocking the gating light is a function of its intensity: the higher the intensity, the stronger the efficiency change. However, the bleaching rate of the first-order grating also increases with increasing gating intensity. The same behavior was observed for transmission (Figure 7A): during the first 60 s, the gating light was blocked and the transmission remains constant as expected. With the gating light on, it decreases abruptly. When the gating light was blocked again, the transmission increases slowly to a fraction of its original value.

Finally, the spatial phase of the grating was intentionally shifted by π during holographic recording by moving the mirror mounted on a piezoelectric transducer (see Figure 2). When the phase shift occurs, the diffraction efficiency increases sharply and then decays rapidly to zero (Figure 8A); on a longer time scale, the growth of a new hologram with smaller diffraction intensity was observed. Phosphorescence and transmission were unaffected by spatial phase shift.

Discussion

If the concentrations of triplet and radical cation are known, the time evolution of the holograms can be easily modeled using

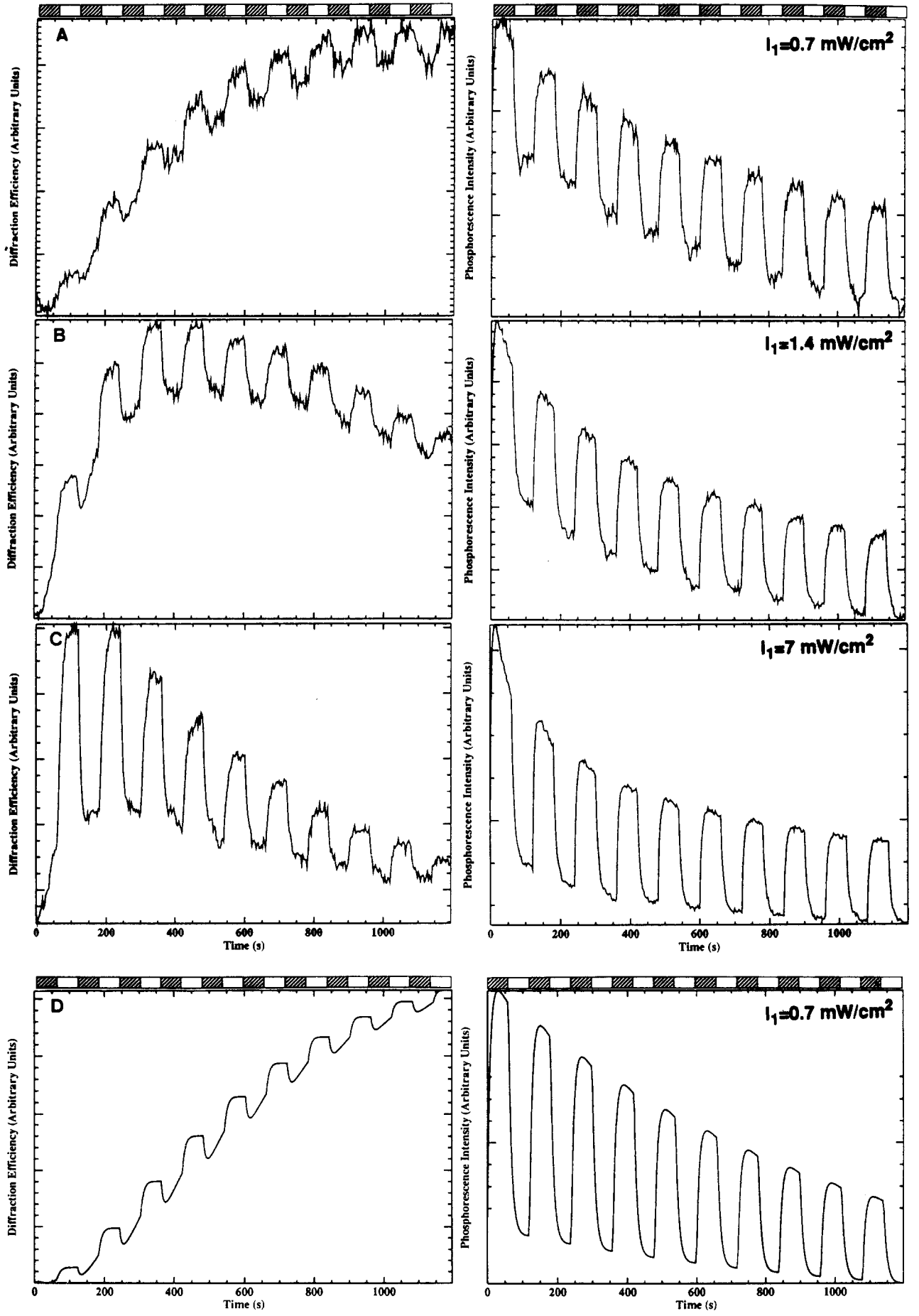

Figure 6. Holographic growth curves read at 363.8 nm and respective phosphorescence with gating light on (dark) and off (white). The intensity of beam 2 was kept constant at 80 mW/cm^2, and gating light (beam 1) intensities were varied. (D) Holographic growth curves and phosphorescence calculated with the same intensities as in (A).

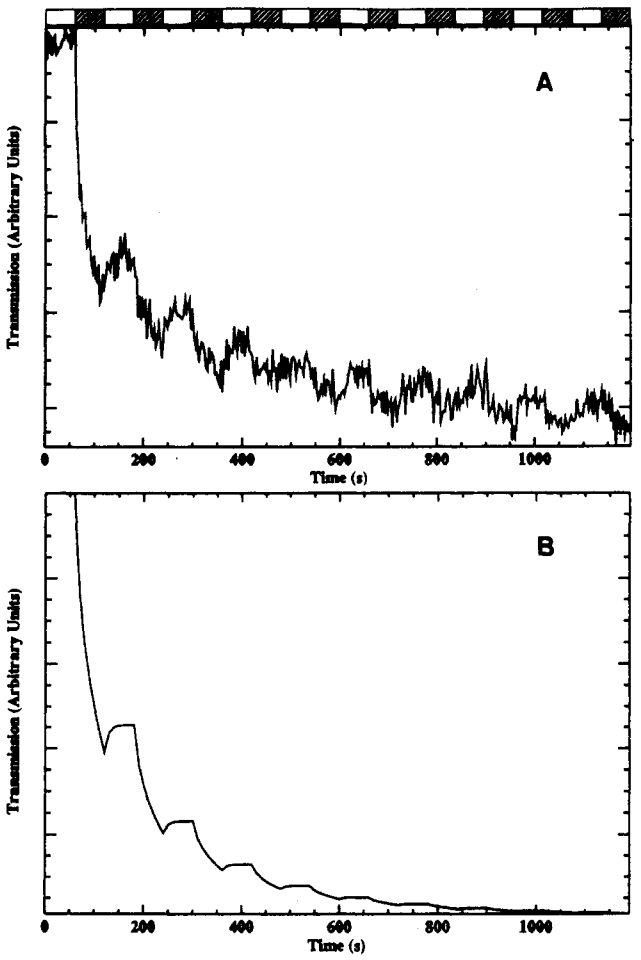

Figure 7. Measured (A) and calculated (B) transmission at 363.8 nm with gating light off (white) and on (dark). I_1 = 6 mW/cm^2, I_3 = 40 mW/cm^2.

eqs 1–5. The reaction scheme for the photoionization of triphenylene in boric acid glass is

$$S_0 \underset{k_{-1}}{\overset{k_1}{\rightleftharpoons}} S_1 \xrightarrow{k_{ISC}} T_1 \underset{k_{-3}}{\overset{k_3}{\rightleftharpoons}} T_n \xrightarrow{k_4} P, \qquad T_1 \xrightarrow{k_2} S_0$$

For easier comprehension of the time evolution of triplet and radical cation populations, the above scheme can be simplified to

$$E \underset{k_2}{\overset{k_1\Phi_{ISC}}{\rightleftharpoons}} I \xrightarrow{k_3\Phi_{ion}} P$$

$$\Phi_{ISC} = \frac{k_{ISC}}{k_{ISC} + k_{-1}} \tag{7}$$

$$\Phi_{ion} = \frac{k_{ion}}{k_{ion} + k_{-3}} \tag{8}$$

where E, I, and P denote, respectively, the educt (S_0), the intermediate (T_1), and the product and Φ_{ISC} and Φ_{ion} are, respectively, the quantum yields of intersystem crossing and of photoionization. k_2 is equal to $1/\tau_0$, τ_0 being the triplet lifetime in the absence of any photochemistry (τ_0 = 10.7 s); k_1 and k_3 depend on excitation intensity and, for optically thin samples, may be expressed as[2]

$$k_1 = 2303\epsilon_S I_1 \tag{9}$$

$$k_3 = 2303\epsilon_T I_2 \tag{10}$$

where ϵ_s and ϵ_T are the molar extinction coefficients of the triphenylene ground and triplet states, respectively, and I_1 and I_2 are the intensities of beam 1 (335 nm) and beam 2 (363.8 nm) (einstein/cm^2·s).

Both rate constants $k_1' = k_1\Phi_{ISC}$ and $k_3' = k_3\Phi_{ion}$ can be deduced from the experimental data. From the above schemes, it is apparent that the observed phosphorescence lifetime τ and k_3' can be related by a Stern–Volmer type equation:

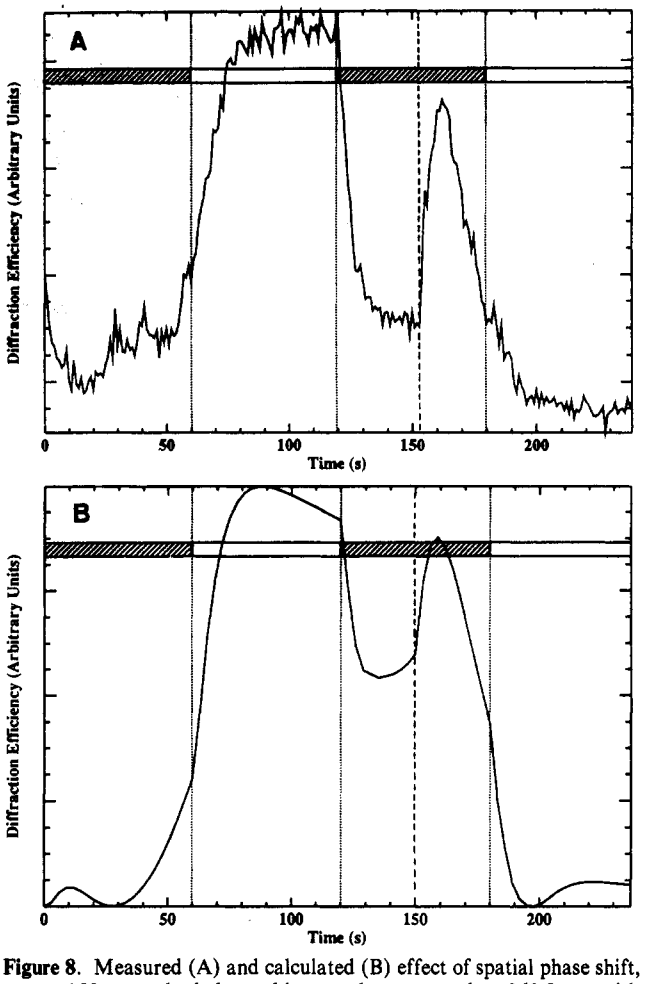

Figure 8. Measured (A) and calculated (B) effect of spatial phase shift, at t = 150 s, on the holographic growth curve read at 363.8 nm with gating light on (dark) and off (white). I_1 = 80 mW/cm^2, I_2 = 6 mW/cm^2.

$$\frac{\tau_0}{\tau} = 1 + \frac{k_3'}{\tau_0} I_2 \tag{11}$$

The measurements of the phosphorescence lifetime τ as a function of the 363.8-nm laser beam intensity I_2 indicate an ion yield Φ_{ion} of about 1.5×10^{-3}.

In the same way, Φ_{ISC} can be deduced from the time t_{max} at which the phosphorescence intensity is maximum:[17]

$$t_{max} = \frac{\ln\left[\dfrac{k_3' + k_2}{k_1'}\right]}{k_3' + k_2 - k_1'} \tag{12}$$

The value of Φ_{ISC} determined in this way is about 0.8, in agreement with the value of the quantum yield of triphenylene fluorescence in hexane, Φ_{fl} = 0.1.[18]

The rate laws describing the simplified reaction scheme are

$$\frac{dC_E}{dt} = -k_1'C_E + k_2C_I \tag{13}$$

$$\frac{dC_I}{dt} = k_1'C_E - (k_2 + k_3')C_I \tag{14}$$

$$\frac{dC_P}{dt} = k_3'C_I \tag{15}$$

(17) Demas, J. N. *Excited State Lifetime Measurements*; Academic Press: New York, 1983.
(18) Berlman, I. *Handbook of Fluorescence Spectra of Aromatic Molecules*; Academic Press: New York, 1971.

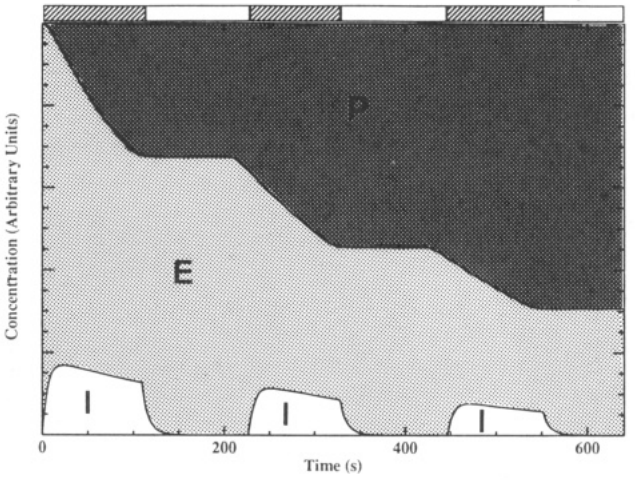

Figure 9. Calculated time evolution of the educt (E, light gray), intermediate (I, white), and product (P, dark gray) concentrations with gating light on (dark) and off (white). $I_1 = 100$ mW/cm^2, $I_2 = 10$ mW/cm^2.

From the above three equations, the time evolution of the intermediate is

$$C_I(t) = A \exp(\lambda_1 t) + B \exp(\lambda_2 t) \quad (16)$$

where A and B are constants and λ_1 and λ_2 the solutions of the following equation:

$$\lambda^2 + (k_1' + k_2 + k_3')\lambda + k_1'k_3' = 0 \quad (17)$$

With $C_I(t=0) = 0$ and with the steady-state approximation, A and B can be determined:

$$C_I\left(t > \frac{1}{k_2 + k_3'}\right) \cong \frac{k_1'}{k_2 + k_3'} C_E \cong \frac{k_1'}{k_2 + k_3'} C_E(t=0) \quad (18)$$

With this approximation, eq 16 becomes

$$C_I(t) = \frac{k_1' C_E(t=0)}{k_2 + k_3'} (\exp(-\lambda_1 t) - \exp(-\lambda_2 t)) \quad (19)$$

The time evolution of the product concentration is

$$C_P(t) \cong C_E(t=0)(1 - \exp(-\lambda_1 t)) \quad (20)$$

When the gating light is switched off at t_0, the reaction becomes

$$E \xleftarrow{k_2} I \xrightarrow{k_3'} P$$

The time dependences of the intermediate and the product are

$$C_I(t) = C_I(t_0) \exp[-(k_2 + k_3')(t - t_0)] \quad (21)$$

$$C_P(t) = C_P(t_0) + \frac{k_3' C_I(t_0)}{k_2 + k_3'} [1 - \exp[-(k_2 + k_3')(t - t_0)]] \quad (22)$$

If the time evolution of intermediate and product concentrations is known (Figure 9), it is then possible to calculate the diffraction efficiency using eqs 1–5.

Figure 4B shows a calculated growth curve with the He–Ne laser as the reading beam; the fit with the experimentally obtained curve (Figure 4A) is good. From these curves, it is not possible to get information on the interference between the E and the P gratings, as this interaction is permanent. On the contrary, the interaction between the I and the E and P gratings vanishes as the population of I decays. At 632.8 nm, the amplitude of the absorbance modulation of I, α_1^I, is much smaller than the amplitude of the absorbance modulation of P, α_1^P. As α_1^E is zero, the total modulation amplitude α_1 is nearly equal to α_1^P. On the other hand, the amplitudes of the refractive index modulation of E, I, and P have almost the same magnitude. Therefore, according to eq 2, the total modulation amplitude of the refractive index n_1 is almost equal to n_1^I, as n_1^E and n_1^P cancel. As a consequence, if the contributions of the phase holograms are as large as the contribution of the amplitude holograms, the phase hologram should disappear when the gating light is removed. As this effect was not observed, the generated holograms must be mostly amplitude holograms. This is further confirmed by the calculation of n_1 and α_1 using eqs 4 and 5 and the values in Table I: at 363.8 nm, the ratio α_1/n_1 is 55 for I and 150 for P, while at 632.8 this ratio is 26 for I and 330 for P.

Figures 6D and 7B show simulations of holographic growth curves read at 363.8 nm and phosphorescence and transmission signals. For long time-scale plots, a correction for the bleaching of the first-order grating has been added; this has been done by considering the triphenylene ground-state concentration to decrease exponentially with irradiation time. At 363.8 nm, the R and ϵ values of I and P are of the same order of magnitude. With gating light on, the amplitude of the absorbance modulation due to the intermediate is of the same order of magnitude as that due to the product. As a consequence, the interaction between the I and P gratings is strong and the total amplitude of the absorption modulation is relatively small; thus, the diffraction efficiency is low. While intermediate concentration is steady and product is continuously formed, diffraction efficiency increases. When the gating light is switched off, the intermediate state population decreases as indicated by the phosphorescence, and the value of α_1^I goes to zero, resulting in an increase of the total modulation amplitude α_1 to the maximum value of α_1^P. Consequently, the diffraction efficiency increases at a rate which is equal to that of the phosphorescence decay. This is confirmed by the transmission signal: the absorbance increases sharply as the gating light is switched on, due to triplet–triplet absorption; when the gating light is turned off, the transmission increases only slightly, as a result of the partial transformation of intermediate to product, the latter having a larger molar extinction coefficient.

After the gating light has been switched off, the phosphorescence does not decay to zero, as might be expected from the reaction scheme depicted at the beginning of this section. In Figure 6 it can be seen that this effect is more pronounced during the first gating on/off sequences. Moreover, the intensity of this residual phosphorescence is independent of the intensity of the gating light. It should also be noted that, during the recording of the phosphorescence, spatially modulated beam 2 is permanently opened. Consequently, this effect is explained by the formation of the triplet state via two-photon excitation by beam 2 to S_1 and via ISC. This has been taken into account in the simulation of the phosphorescence signal by adding the E concentration, multiplied by the probability of two-photon absorption, to the triplet population generated via single-photon excitation. With this correction, the observed phosphorescence signals are well reproduced.

Finally, Figure 8B shows the calculated holographic growth curve read at 363.8 nm with an intentional π phase shift at time $t_{ps} = 150$ s. Neglecting the contribution of the refractive index gratings, the effect of the phase shift can be rationalized as follows: when gating light is turned on for the second time, a well-formed P grating is already present. As the concentration of I increases, its grating builds, counterbalancing the effect of the P grating; the diffraction efficiency decreases. When the phase between the two interfering beams is shifted by π, new P and I gratings are created with a phase difference of π relative to the old ones. The total amplitude of the absorbance modulation is now

$$\alpha_1 = \alpha_1^{Pold} + \alpha_1^{Iold} - \alpha_1^{Pnew} - \alpha_1^{Inew} \quad (23)$$

After the phase shift, the positive contributions to α_1 result from the old P grating ($\alpha_1^{Pold} > 0$) and from the new I grating ($\alpha_1^{Inew} < 0$). The negative contribution to α_1 originates from the old I grating ($\alpha_1^{Iold} < 0$) and the new P grating ($\alpha_1^{Pnew} > 0$). It should be noted that, after the phase shift, α_1^{Pold} remains constant while α_1^{Iold} decays:

$$\alpha_1^{Iold}(t - t_{ps}) = \alpha_1^{Iold}(t_{ps}) \exp[-(k_2 + k_3')(t - t_{ps})] \quad (24)$$

where t_{ps} is the time at which the phase shift occurs. This relation explains why the hologram efficiency increases very quickly just after the externally induced phase shift. After some time, α_1^{Pnew} increases sufficiently to reduce α_1 to zero; hence, the total dif-

fraction efficiency drops to zero. Later, as the new product concentration grating increases even more, α_1 becomes negative. As a consequence, the total diffraction efficiency starts to rise again, $\sinh^2$ being an even function (see eq 1).

Conclusion

Boric acid glass doped with triphenylene is well suited for gated hologram recording at low light intensities of the order of a few mW/cm^2. The measured diffraction efficiencies are small due first to the low concentration of the active compound (10^{-3} M) in the matrix and second to the wavelengths at which the holograms are read. Higher diffraction efficiencies can probably be obtained with higher dopant concentrations and by reading the holograms at a wavelength corresponding to the absorption maximum of the product.

In the present paper, we also showed the importance of the wavelength of the reading beam on the diffraction efficiency. In order to obtain higher holographic efficiency, the magnitude of absorption coefficient and molar refraction of educt and product at the reading wavelength should be as different as possible. Either the absorption coefficient and molar refraction of product should be much larger than those of the educt when the product concentration grating dominates or those of the product should be much smaller that those of the educt when the holographic efficiency results from the educt concentration grating. Intermediate cases, where the magnitudes of product and educt absorption coefficients and molar refraction are similar, lead to a complicated behavior. This does not apply for intermediate states like the triplet state, whose contribution vanishes if this state is not continuously repopulated. On the other hand, such interference between product, educt, and intermediate state gratings can give valuable information on the dynamics and the kinetics of the reacting systems, information which sometimes cannot be obtained through conventional methods.

Acknowledgment. We express our thanks to Dr. F. A. Burkhalter for his invaluable help during the early phases of the experimental work and to Dr. A. Renn and Dr. K. Holliday for helpful discussions. This work was supported by the Swiss National Science Foundation.

Keto–Enol Tautomerization of 2-(2′-Hydroxyphenyl)benzoxazole and 2-(2′-Hydroxy-4′-methylphenyl)benzoxazole in the Triplet State: Hydrogen Tunneling and Isotope Effects. 1. Transient Absorption Kinetics

Wajih Al-Soufi, Karl H. Grellmann,* and Bernhard Nickel

Max-Planck-Institut für Biophysikalische Chemie, Abt. Spektroskopie, Am Fassberg, W-3400 Göttingen, Germany *(Received: August 1, 1991)*

Hydrogen tunnel effects in the metastable triplet states of 2-(2′-hydroxyphenyl)benzoxazole (HBO) and 2-(2′-hydroxy-4′-methylphenyl)benzoxazole (*m*-MeHBO) and their deuteriooxy analogues DBO and *m*-MeDBO have been investigated between 35 and 250 K in three alkane solvents that have drastically different viscosities at low temperatures. In the triplet states of HBO the hydrogen transfer between the enol and keto tautomers is reversible because the two triplet states are isoenergetic. In *m*-MeHBO the hydrogen transfer is virtually unidirectional because the initially populated keto triplet state has a higher energy than the enol triplet state. In spite of these differences the observed hydrogen-transfer rate constants of the two compounds have nearly the same values. The temperature dependence of the rate constants is insensitive to large changes in solvent viscosity, i.e., hydrogen tunneling in HBO and *m*-MeHBO depends on solvent friction neither at intermediate nor at very low temperatures. The couples HBO, DBO and *m*-MeHBO, *m*-MeDBO are the first examples where the determination of tunneling rate constants has been extended for both isotopomers into a temperature region where the rates and the isotope effect on these rates become temperature independent.

I. Introduction

For the study of light-induced hydrogen- or proton-transfer processes 2-(2′-hydroxyphenyl)benzoxazole (HBO) is a very interesting compound because it can exist in two tautomeric forms, the enol tautomer (E) and the keto tautomer (K), whose relative stabilities depend on their electronic state. In the electronic ground state of HBO the enol form, ^{1}E, is the stable tautomer. In its first excited singlet state, ^{1}E*, very rapid adiabatic proton transfer takes place,[1] yielding the first excited singlet state of the keto tautomer, ^{1}K*, whose energy is 2100 cm^{-1} lower[2] than that of ^{1}E*.

^{1}K* is depopulated by thermally activated internal conversion and fluorescence to the keto singlet ground state, ^{1}K, and by intersystem crossing to the keto triplet state, ^{3}K*.[3] The keto tautomer is in its singlet ground state less stable than ^{1}E (energy difference 4900 cm^{-1})[2] and decays therefore rapidly to ^{1}E. The quantum yield of intersystem crossing from ^{1}E* to the enol triplet state, ^{3}E*, is virtually zero because of the ultrafast proton transfer

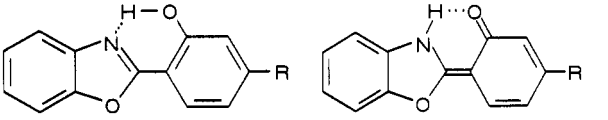

E E_m K K_m

R = H: HBO

$R = CH_3$: m-MeHBO

^{1}E* ⇝ ^{1}K*. This initial population of the *keto* triplet state is a very interesting photophysical property of HBO, because it allows one to study the kinetics of a hydrogen-transfer reaction in the metastable triplet state: We have shown recently[4] that after the formation of ^{3}K*, which takes place within a few nanoseconds, the equilibrium $^3K^* \rightleftharpoons {}^3E^*$ is established between the keto and enol triplet state (Scheme I). Below ~200 K, the rate constants of this reaction are predominantly determined by hydrogen tunnel

(1) Woolfe, G. J.; Melzig, M.; Schneider, S.; Dörr, F. C. *Chem. Phys.* **1983**, *77*, 213 and references therein.
(2) Rodriguez Prieto, M. F.; Nickel, B.; Grellmann, K. H.; Mordziński, A. *Chem. Phys. Lett.* **1988**, *146*, 387.
(3) Mordziński, A.; Grellmann, K. H. *J. Phys. Chem.* **1986**, *90*, 5503.
(4) Grellmann, K. H.; Mordziński, A.; Heinrich, A. *Chem. Phys.* **1989**, *136*, 201.

0022-3654/91/2095-10503$02.50/0